Converting Phenylacetone Monooxygenase into Phenylcyclohexanone Monooxygenase by Rational Design

Bocola, Marco; Schulz, Frank; Leca, François; Vogel, Andreas; Fraaije, Marco W.; Reetz, Manfred T.

Published in:
Advanced Synthesis & Catalysis

DOI:
10.1002/adsc.200505069

Converting Phenylacetone Monooxygenase into Phenylcyclohexanone Monooxygenase by Rational Design: Towards Practical Baeyer–Villiger Monooxygenases

Marco Bocola,[a] Frank Schulz,[a] François Leca,[a] Andreas Vogel,[a] Marco W. Fraaije,[b] Manfred T. Reetz[a,*]

[a] Max-Planck-Institut für Kohlenforschung, Kaiser-Wilhelm-Platz 1, 45470 Mülheim/Ruhr, Germany
Fax: (+49)-208-306-2985, e-mail: reetz@mpi-muelheim.mpg.de
[b] Rijksuniversiteit Groningen, Department of Biochemistry, Nijenborgh 4, 9747 AG Groningen, The Netherlands
E-mail: m.w.Fraaije@rug.nl

Received: February 1, 2005; Accepted: March 21, 2005

Abstract: A homology model of the most frequently used, but thermally somewhat labile, Baeyer–Villiger monooxygenase, cyclohexanone monooxygenase (CHMO) has been derived on the basis of the recently published crystal structure of the thermally stable phenylacetone monooxygenase (PAMO). This has led to the identification of a structural element crucial for substrate acceptance and stereoselectivity, namely an arginine-interacting loop near the active site. A bulge in this loop occurring in PAMO (but not in CHMO) has been eliminated by mutation, enhancing the range of substrate acceptance and enantioselectivity of Baeyer–Villiger reactions while maintaining high thermal stability.

Keywords: asymmetric catalysis; enzymes; molecular modeling; oxidation; protein engineering; protein structures

Introduction

The Baeyer–Villiger (BV) reaction of ketones with formation of the corresponding esters or lactones is an important transformation in synthetic organic chemistry.[1] It can be catalyzed by acids, bases, metal complexes or flavin-dependent enzymes. The latter are generally called Baeyer–Villiger monooxygenases (BVMOs),[2] an example of which are the cyclohexanone monooxygenases (CHMOs).[2,3] It has been shown that in this enzymatic process dioxygen (air) reacts with the reduced enzyme-bound flavin (FAD) to form an intermediate peroxide-anion which, in the deprotonated form, initiates the BV reaction by nucleophilic addition to the carbonyl function.[2,3] This process leads to the so-called Criegee intermediate which then rearranges to the ester (or lactone). Ultimately O_2 delivers one oxygen atom to the substrate, the other being reduced to water (Scheme 1). The oxidized flavin then needs to be recycled by reduction, the coenzyme NADPH taking over this function. Therefore, when employing the isolated CHMOs, NADPH itself has to be recycled. For this reason organic chemists have found it more convenient to use whole cells.[2–4] Employing CHMO-containing strains from various organisms, this procedure has been applied successfully in the kinetic resolution of a variety of different chiral ketones and in the desymmetrization of various prochiral substrates (often > 90% ee).[3,4] Of course, substrate acceptance and enantioselectivity are by nature limited. For this reason we recently extended the synthetic value of this biocatalytic process by applying the methods of directed evolution in order to control the degree and direction of enantioselectivity.[5] In that study whole-cell preparations of *E. coli* expressing the recombinant CHMO[6] from *Acinetobacter* sp. NCIMB 9871 were used.[5] However, due to the fact that at that time not a single BVMO had been structurally characterized by X-ray crystallography, it was not possible to relate the results to a molecular basis.

Most recently, Malito, Alfieri, Fraaije and Mattevi reported the first crystal structure of a BVMO.[7] The so-called phenylacetone monooxygenase (PAMO) from the moderately thermophilic bacterium *Thermobifida fusca*, discovered previously by genome mining,[8] was shown to exhibit a two-domain architecture resembling structural characteristics of disulfide oxidoreductases. The crystal structure reveals a cleft at the domain interface, at which the active site is located. Arginine at position 337 was identified above the bound flavin ring in a position ideally suited to stabilize the negatively charged flavin peroxide.[7] Two further points deserve mention: Firstly, this BVMO is the thermally most robust of its kind known to date, making it an attractive candidate for potential application in organic chemistry. Sec-

 DOI: 10.1002/adsc.200505069

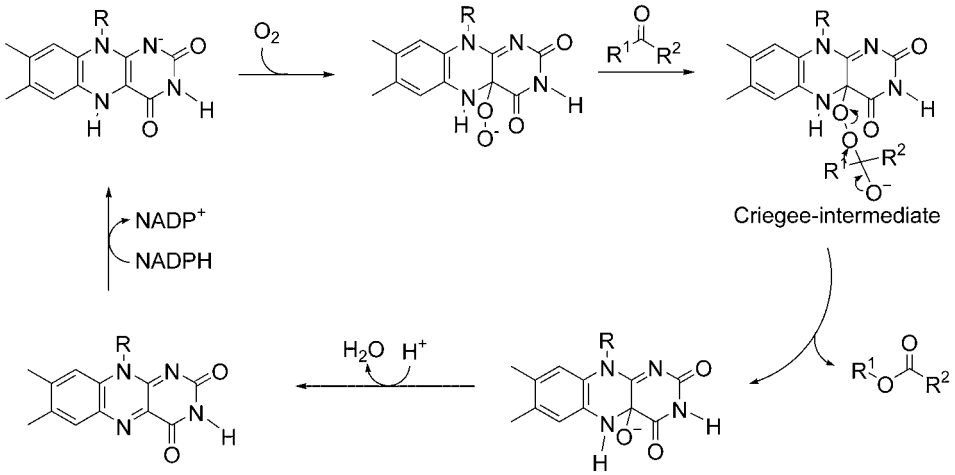

Scheme 1. Schematic representation of BVMO-catalyzed Baeyer–Villiger reactions of ketones.

ondly, of various ketone substrates tested in the BV reaction, phenylacetone was shown to be oxidized most rapidly.[8] PAMO appears to prefer substrates bearing phenyl groups, although it is currently not possible to define the pocket in which the aromatic moiety binds. In contrast, ketones such as cyclohexanone are not accepted or react extremely slowly.[8] Thus, PAMO has the attractive feature of being unusually stable, but its range of substrate acceptance is rather limited and enantioselectivity is low.[8]

In Mülheim we became interested in the crystal structure of PAMO because it allowed us to construct a structural model of the wild-type (WT) CHMO and the highly enantioselective mutants that we had created earlier by directed evolution.[5] Moreover, another point of interest emerged, which is the subject of the present study. Upon comparing the CHMO homology model with the crystal structure of PAMO, a remarkable structural *difference* became apparent, namely the presence of a bulge in the loop near the active site of PAMO which is absent in CHMO (see below). One can imagine that the presence of this bulge places limits on the range of substrate acceptance of PAMO. Therefore, full or partial elimination of the bulge could turn the PAMO into an enzyme variant displaying an enlarged substrate acceptance while maintaining its thermal stability. This inspired us to perform "rational" engineering of PAMO with the aim of obtaining a "phenylcyclohexanone monooxygenase" (PCHMO). Indeed, 2-phenylcyclohexanone is a substrate that is hardly accepted by the WT PAMO.

Results and Discussion

Homology Model of CHMO

In order to generate a structural model of CHMO based on the crystal structure of PAMO (pdb-code 1W4X), we applied the CBS-CPHmodels-2.0 3D-homology modeling server.[9] The sequence identity of the CHMO (523 amino acids) and PAMO (524 amino acids) is 40.3%, and the calculated BLAST-alignment score is 526. Figure 1 shows a portion of the CHMO/PAMO alignment focusing on the differences in the arginine-interacting loops of the two enzymes.

All conserved motifs typical of flavin and nicotinamide cofactor binding sites and other known sequence motifs for monooxygenases[10] are correctly aligned, which speaks for the reliability of the predicted 3D model. Figure 2 (top) shows the overall fold of PAMO and the CHMO homology model. As already mentioned in the introduction, the most prominent structural difference between PAMO and CHMO is the presence of an additional bulge in one of the loops of PAMO. The bulge is defined by Ser-441, Ala-442 and Leu-443 (compare Figure 1). This loop occurs in the FAD-binding domain and is spatially located next to the catalytic arginine (Arg-337) (Figure 2, bottom). As delineated below, Arg-337 is instrumental in stabilizing the negatively charged flavin peroxide intermediate. Our previous work concerning the directed evolution of enantioselective BV monooxygenases showed that position 432 of CHMO is one of the important hot spots, and we now

Figure 1. Differences in the arginine-interacting loop between PAMO and CHMO. Excerpt of the sequence alignment between PAMO and CHMO. Identical residues are shaded black and homologous residues are in gray. The blue box surrounds the arginine-interacting loop. The amino acids that were mutated in this study are colored red.

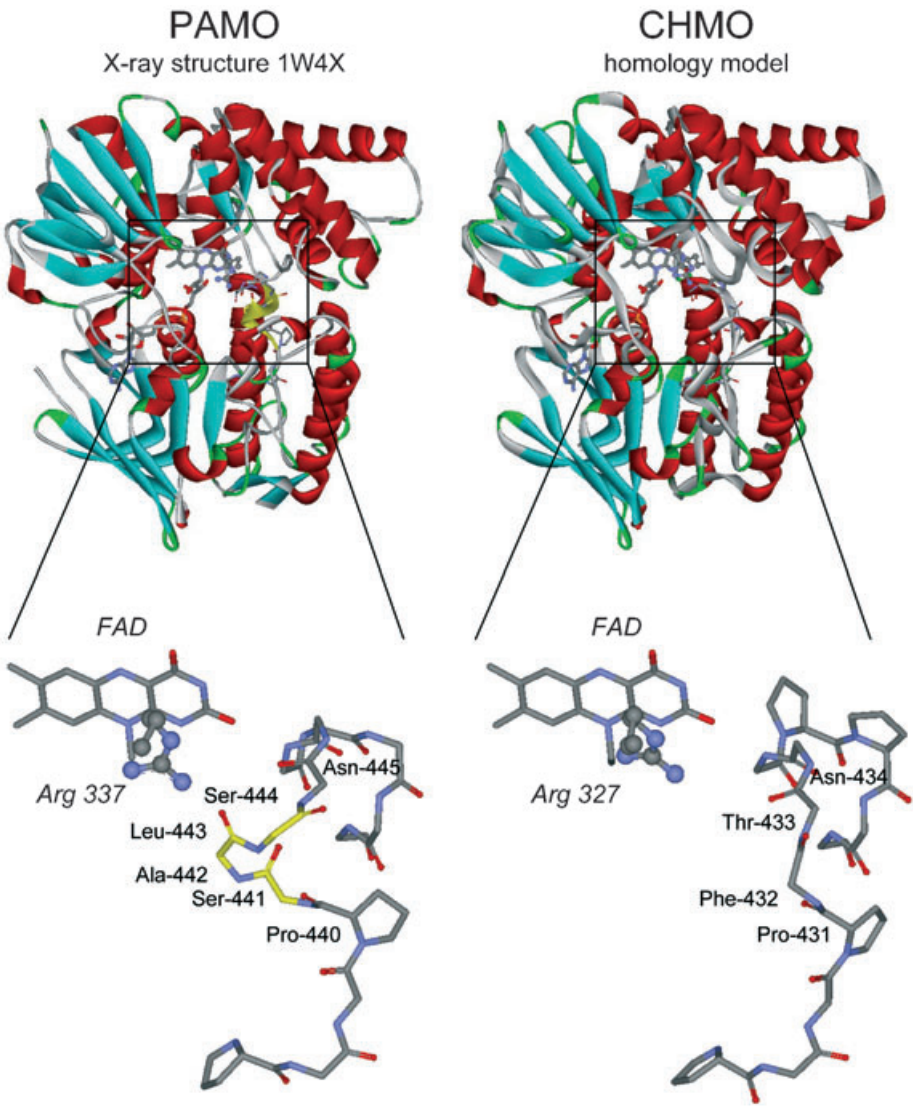

Figure 2. Comparison of the crystal structure 1W4X of PAMO (left) and the homology model of CHMO (right) with 40.3% sequence identity. The upper part shows the overall fold and the lower part is a zoom into the active site showing the FAD cofactor as solid sticks and the catalytic arginine in ball-and-stick model. The yellow color highlights the presence of two additional amino acids in the arginine-stabilizing loop of PAMO compared with CHMO drawn as a backbone representation.

know that it occurs in the corresponding (shorter) arginine-interacting loop. Mutations at this position have a dramatic influence on the direction and magnitude of enantioselectivity of BV reactions[5] and sulfoxidation of prochiral thioethers.[11] In our homology model of CHMO Phe-432 occurs at the position corresponding to Leu-443 at the start of the bulge in PAMO (for alignment see blue box in Figure 1).

Mutational Studies at the Bulge of PAMO

Our immediate goal was to generate three PAMO variants by manipulating the bulge in the arginine-interacting loop in the following way:

- P1: deletion of Ala-442,
- P2: deletion of Ala-442 and Leu-443, and
- P3: deletion of Ser-441 and Ala-442.

The enzyme variants were generated by Quick-Change PCR from the pPAMO-vector described elsewhere and expressed in *E. coli* TOP10-cells (see Experimental Section).[8]

Catalytic Profile of the PAMO Variants

We initiated the study of substrate acceptance by subjecting phenylacetone (**1**) and 2-phenylcyclohexanone (**3**) to the BV reaction using the purified PAMO variants

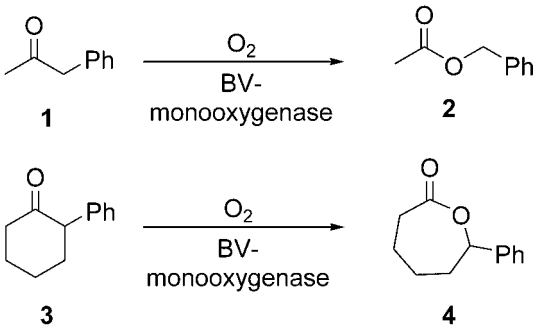

in the presence of defined amounts of NADPH. Enzyme activity was determined by UV/Vis spectroscopy by monitoring the decrease in NADPH concentration, which is conveniently possible by measuring the decrease in characteristic absorbance at 340 nm. All experiments were performed at 25 °C using air-saturated Tris-HCl buffers according to a modified literature procedure.[8]

The steady-state kinetic parameters (Michaelis–Menten) are summarized in Table 1. It can be seen that the catalytic profile is clearly changed by deleting the bulge from the arginine-interacting loop. A cyclohexanone derivative such as 2-phenylcyclohexanone (**3**), which is hardly turned over by the WT PAMO with a conversion barely reaching 10% in whole-cell catalysis within 24 hours (see below), shows almost full conversion with, for example, mutant P3 as catalyst. Mutant P3 has a K_M value of 0.07 mM for 2-phenylcyclohexanone (**3**), comparable to the K_M of 0.059 mM observed for the WT PAMO with respect to phenylacetone (**1**).[8] The conversion of 2-phenylcyclohexanone (**3**) by mutant P2, the second PAMO variant with the size of the arginine-positioning loop being reduced to the size of the corresponding loop in CHMO, is comparable to mutant P3. Its K_M towards this substrate is 0.5 mM. This indicates that steric constraints applied by the arginine-interacting loop play a major role in the substrate binding by the enzyme. The significant differences in K_M values between mutants P2 and P3, on the other hand, suggest further interactions that cannot be readily explained at this time.

While increasing the affinity for cyclohexanone derivatives by deleting the bulge, the catalytic efficiency in the oxidation of the parent substrate phenylacetone (**1**) is actually decreased. Although we could get high conversions in whole-cell catalysis, the K_M values for all three generated PAMO variants are significantly increased over that of the WT enzyme. Importantly, the thermostability of the new PAMO variants is comparable to that of the wild-type and was determined at 50 °C. For variant P1 we found a half-life time of 29 h ± 2 h with a free energy for the denaturation of 105.3 kJ/mol ± 0.5 kJ/mol, for variants P2 and P3 half-life times of 16 h ± 3 h (103.7 kJ/mol ± 0.5 kJ/mol) and 17 h ± 2 h (103.9 kJ/mol ± 0.5 kJ/mol), respectively. These half-life times are comparable to those measured for the wild-type enzyme.[8]

We then turned to the use of whole cells and expanded the list of substrates to include ketones **5**–**8**. The results show that, under the conditions used, only those ketones undergo BV reactions that have a phenyl group near the carbonyl function, namely **1**, **3** and **7**. In contrast, cyclohexanone (**5**), 4-phenylcyclohexanone (**6**) and progesterone (**8**) do not react to any appreciable extent.

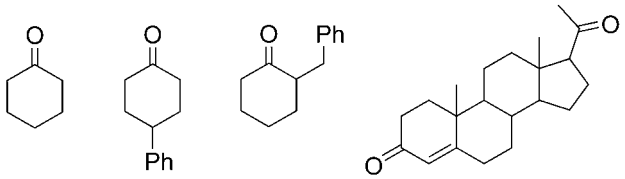

Compounds **3** and **7** are chiral, which offers the opportunity to study kinetic resolution. Although the WT PAMO requires very long reaction times for reasonable conversion, it was included in the study. Table 2 shows the conversions and enantioselectivities obtained in whole-cell catalysis of ketones **3** and **7**. WT PAMO oxi-

Table 1. Steady-state kinetic parameters of WT PAMO and variants.

Substrate	PAMO variant	K_M [mM]	k_{cat} [s^{-1}]	k_{cat}/K_M [$M^{-1} s^{-1}$]
1	WT[a]	0.059	1.9	32000
1	P1	3 ± 1	0.25 ± 0.02	82
1	P2	4 ± 2	0.40 ± 0.04	99
1	P3	2.5 ± 0.4	0.22 ± 0.01	89
3	WT	n.d.	n.d.	n.d.
3	P1[b]	2.3 ± 0.5	0.31 ± 0.03	134
3	P2[b]	0.5 ± 0.1	0.5 ± 0.2	1054
3	P3[b]	0.07 ± 0.01	0.25 ± 0.02	3395

[a] Literature value measured without addition of acetonitrile.[8]
[b] A racemic mixture was used.

dizes ketone **3** with low conversions and essentially no stereoselectivity, whereas we observed increasing conversions in the case of the mutants in the order P1 < P2 < P3. The most active PAMO variant P3 also shows excellent stereoselectivity in the kinetic resolution of ketone **3**. An *E* value of 100 at 50% conversion was obtained after 2 h of reaction in favor of (*R*)-**4**. Significantly, the WT CHMO also shows (*R*) selectivity in this kinetic resolution with an *E*-value of > 100.[12] However, as already pointed out its thermal stability is fairly low. Thus, mutant P3 is characterized by the thermal stability of WT PAMO and the high enantioselectivity of WT CHMO.

Conversion of substrate **7** is in general less efficient than that of substrate **3**. It is significantly converted only by mutant P3. In this reaction only one enantiomeric form of lactone **9** could be detected by chiral GC at a conversion of 40% ($E > 200$) in favor of the (*R*)-product, which again is similar to the oxidation by the WT CHMO.

Since in our previous work concerning the directed evolution of CHMOs we had discovered that certain mutants are not only excellent catalysts for asymmetric BV reactions,[5] but also for enantioselective oxidations of prochiral thioethers,[11] we decided to test the PAMO variants in the sulfoxidation of thioether **10**.[4f–m] PAMO variant P3 turned out to be quite enantioselective, leading to an ee value of 90% in favor of the (*R*)-**11**. For comparison, WT PAMO and CHMO give an ee value of 79.5% and 14%, respectively.

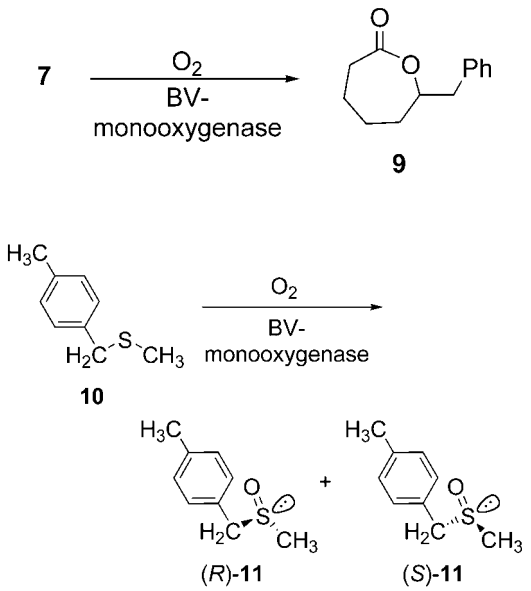

Molecular Modeling of the Criegee Intermediate

We compared the structure of the active sites and analyzed the differences by modeling the Criegee intermediate arising from the reaction of 2-phenylcyclohexanone (**3**) into the PAMO crystal structure and the created CHMO homology model using the united atom force field MAB as implemented in MOLOC with implicit solvation.[13] The structures were subsequently minimized and relaxed by molecular dynamics to analyze the geometry of the active site with bound substrate according to a procedure described previously.[13c] This was required because we started from an experimental crystal structure without bound ligand. This exploratory modeling shows that a difference in the arginine-interacting loop between PAMO and CHMO, namely the bulge defined by Ser-441, Ala-442 and Leu-443 in PAMO, sterically constrains Arg-337 and thus prevents conversion of cyclic ketones.

We then modeled the substrate **3** into the PAMO variant P3 in which Ser-441 and Ala-442 are deleted. Figure 3 shows that a shortening of this active site loop by two amino acids leads to a PAMO variant which is able to bind 2-phenylcyclohexanone (**3**) in the form of a Criegee intermediate, the latter being stabilized by H-bonding to Arg-337 (Figure 3). In sharp contrast, the WT PAMO does not provide enough space in the active site to position substrate **3** in the form of a Criegee intermediate due to the presence of the bulge. Thus, we propose that the nature of the arginine-interacting loop (Figure 2) is responsible for the different substrate recognition when going from linear ketones like phenylacetone (**1**) to cyclic ketones like 2-phenylcyclohexanone

Table 2. Kinetic resolution of ketones **3** and **7** using whole cells.

Ketone	Enzyme variant	E[a]	% conversion after 24 h	Preferred enantiomer
3	WT-PAMO	1.2	10	*S*
3	P1	35	51	*R*
3	P2	23	72	*R*
3	P3	100	91	*R*
7	WT-PAMO	–	0	–
7	P1	–	0	–
7	P2	–	0	–
7	P3	> 200	40	*R*

[a] *E*-values were calculated on the basis of 40–50% conversion (except for the WT).

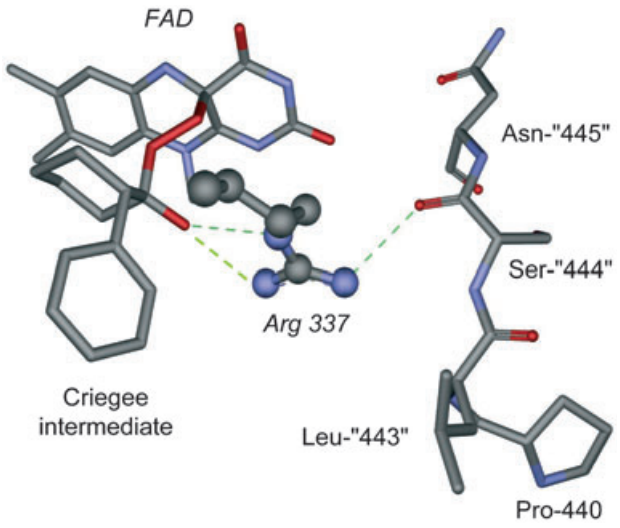

Figure 3. Model of the PAMO variant P3 with deleted Ser-441 and Ala-442 containing the Criegee intermediate arising from 2-phenylcyclohexanone (**3**) in a reactive geometry with two H-bonds originating from the catalytic Arg-337.

(**3**). The reason for the necessity of phenyl groups near the carbonyl function still needs to be clarified.

Conclusions

Since the early work of Taschner[4a] describing the application of Baeyer–Villiger monooxygenases as catalysts in organic chemistry, a number of other synthetic organic chemists have exploited these enzymes in asymmetric transformations, usually employing a CHMO in the form of whole cells.[2–4] In spite of the pioneering mechanistic work of a number of biochemists,[2] detailed interpretations of asymmetric BV reactions have not been possible due to the long-standing problem of obtaining suitable crystals of these relatively unstable enzymes, making crystallographic characterization impossible. For this reason all published models of the stereochemical outcome of enzyme-catalyzed BV reactions constitute useful mnemonic devices,[3,4,14] but they really do not include structural aspects on a molecular basis. The recently published crystal structure of a thermostable Baeyer–Villiger monooxygenase PAMO[7] has changed the situation. PAMO has a relatively narrow range of substrate acceptance, but it is thermally robust.[8] In the present study we have utilized the structural information in order to construct a homology model of the widely used CHMO. As a result we have been able to apply molecular modeling, which has emerged in the identification of a structural element essential in enzyme-catalyzed BV reactions: the arginine-interacting loop, as shown in Figures 1 and 3. The presence of this loop seems to be conserved throughout BVMOs. We have shown that manipulation of this structural element strongly influences substrate acceptance and enantioselectivity.

The comparison of the crystal structure of the WT PAMO with the CHMO homology model allowed us to rationally redesign the PAMO with the goal of expanding the range of its substrate acceptance while maintaining thermal stability. The PAMO was successfully turned into a phenylcyclohexanone monooxygenase (PCHMO). This was accomplished by deleting major parts of a bulge occurring in the arginine-interacting loop near the active site. The observation that fast turnover requires the presence of a phenyl group near the carbonyl function of the ketone substrate illuminates the scope and limitation of the present PAMO variants. This structural feature is currently difficult to explain, and we refrain from unfounded speculations. Nevertheless, on the practical side the developments described in this study can be considered to be steps towards the ultimate goal of creating thermostable BV monooxygenases showing broad substrate acceptance and high degrees of enantioselectivity. One logical approach would be to perform saturation or cassette mutagenesis[15] in the arginine-interacting loop. Finally, the structural and mechanistic information emerging from the present study is helping us in the interpretation of the results of our previous investigation concerning the directed evolution of enantioselective CHMOs.[5,11] One of the mutations occurring at an important "hot spot" responsible for enhanced stereoselectivity was reported to be F432S, which we can now identify as being in the loop near the active site. Ser-432 probably forms a hydrogen bond with the catalytically active arginine. More detailed theoretical and experimental studies are in progress.

Experimental Section

Materials

Phenylacetone (**1**), 2-phenylcyclohexanone (**3**), cyclohexanone (**5**), 4-phenylcyclohexanone (**6**), 2-benzylcyclohexanone (**7**) and progesterone (**8**) were obtained from Aldrich and Fluka. *p*-Methylbenzyl methyl sulfide was synthesized using a procedure described in the literature. Racemic lactones for GC analysis were synthesized by *m*CPBA oxidation of the ketones. NADPH was obtained from Jülich Fine Chemicals. DNA sequencing was done at Medigenomix (Martinsried, Germany).

Mutation and Expression of Recombinant PAMO

pPAMO was purified from *E. coli* TOP10 cells using the QIAprepr Spin Miniprep Kit and subjected to Quick-Change PCR following the Stratagene Quick-Change-Kit protocol (Stratagene) with HotStart KOD-Polymerase (Novagen) using the following primers:

P1-fw: 5′-aggcccgggcagcccgtctctcagcaacatgctggtct-3′, P1-rev: complementary to P1-fw,

P2-fw: 5′-aggcccgggcagcccgtctagcaacatgctggtctcta-3′, P2-rev: complementary to P2-fw,

P3-fw: 5′-gcaggcccgggcagcccgctcagcaacatgctggtc-3′, P3-rev: complementary to P3-fw.

The resulting plasmids were transformed into *E. coli* TOP10. Integrity of the coding region was verified by DNA sequencing. For expression the cells were cultivated in either LB-Medium (for whole-cell catalysis) or TB-Medium (for purification of the PAMO variants) supplemented with 0.1% L-arabinose and 100 μg/mL carbenicilline at a temperature of 37 °C.

Purification of Recombinant PAMO Variants

Purification of the PAMO variants was performed as described elsewhere for WT PAMO with minor modifications.[8]

Steady-State Kinetics

Protein concentrations were measured photometrically by monitoring the absorption of the FAD-cofactor at 441 nm ($\varepsilon_{441} = 12.4\ mM^{-1}\ cm^{-1}$). For steady-state kinetics purified PAMO mutants at a concentration of 1 μM were dissolved in 50 mM Tris-HCl (pH 8.0) in the presence of 100 μM NADPH. Substrates were dissolved in acetonitrile and added to the premixed enzyme solution resulting in an acetonitrile concentration of 2.5% (v/v). NADPH consumption was continuously measured at 340 nm ($\varepsilon_{340} = 6.22\ mM^{-1}\ cm^{-1}$). The kinetics were measured at 25 °C. The obtained data were fitted to the Michaelis–Menten equation by non-linear regression analysis implemented in the program Origin 7.0 (Microcal, Northampton, MA). For measuring the thermostability of the PAMO variants, solutions of the purified enzymes were incubated at 50 °C. Activity was determined as described above in the presence of 20 mM phenylacetone (substrate saturation conditions). The data were fitted to a single exponential decay curve using Origin 7.0 and the half-life time was calculated. The free energy of denaturation was calculated from the deactivation rate k_d using the formula:

$$\Delta G = -RT \ln\left[k_d h / k_B T\right].$$

Whole-Cell Catalysis

For whole cell catalysis TOP10-expression cultures in LB-Medium were grown to an OD_{600} of 2.5–3.0 and subsequently supplemented with 5 g/L of glycerol. The PAMO variants were heat-activated at 45 °C (15 min for 20 mL of culture). Afterwards the biocatalytic reactions were started as described below.

Baeyer–Villiger Oxidation of 2-Phenylcyclohexanone (3) and 2-Benzylcyclohexanone (7)

20 mL of heat-treated TOP10-expression culture were mixed with 280 μL of a 0.1 M solution of 2-phenylcyclohexanone (**3**) or 2-benzylcyclohexanone (**7**), respectively, in acetonitrile. In the case of 2-benzylcyclohexanone (**7**) 1 mL of a solution of 2-hydroxypropyl-β-cyclodextrin (Wacker CAVASOL W7 HP Pharma, 134.3 mg/mL in water) was added for solubilization. The culture was further grown at 37 °C in 100-mL Erlenmeyer flasks. Samples were taken at various time intervals and extracted with 2 equivalents of ethyl acetate and subsequently analyzed by chiral GC (column and condition: 30 m BGB 177 and BGB 15 column, respectively, 0.25 mm i.d., 0.25 μm film; G/468; 0.5 bar hydrogen pressure, 76 min isotherm 130 °C, 25 min, isotherm 200 °C, 15 min). The assignment of absolute configuration of the resulting lactones is based on literature data.[12] In the case of kinetic resolution, the formula of Sih[16] was used to obtain the *E* values.

Sulfoxidation of *p*-Methylbenzyl Methyl Sulfide (10)

20 mL of heat-treated TOP10-expression culture were mixed with 15 μL of neat *p*-methylbenzyl methyl sulfide (**10**) and 3 mL of a solution of 2-hydroxypropyl-β-cyclodextrin (Wacker CAVASOL W7 HP Pharma, 134.3 mg/mL in water) were added. The culture was further grown at 30 °C and extracted with 2 equivalents of dichloromethane and analyzed by chiral HPLC as previously described.[11]

Acknowledgements

We thank Silvia Ruthe and Heike Hinrichs for help with the chromatographic work. Support by the Fonds der Chemischen Industrie is gratefully acknowledged.

References and Notes

[1] a) G. R. Krow, *Org. React. (N. Y.)* **1993**, *43*, 251–798; b) M. Renz, B. Meunier, *Eur. J. Org. Chem.* **1999**, 737–750; c) G. Strukul, *Angew. Chem.* **1998**, *110*, 1256–1267; *Angew. Chem. Int. Ed.* **1998**, *37*, 1198–1209; d) C. Bolm, T. K. K. Luong, O. Beckmann, in: *Asymmetric Oxidation Reactions*, (Ed.: T. Katsuki), University Press, Oxford, **2001**, p. 147.

[2] Isolation, characterization and/or mechanistic studies of CHMOs as whole cells or isolated enzymes: a) G. E. Turfitt, *Biochem. J.* **1948**, *42*, 376–383; b) N. A. Donoghue, D. B. Norris, P. W. Trudgill, *Eur. J. Biochem.* **1976**, *63*, 175–192; c) J. M. Schwab, W. B. Li, L. P. Thomas, *J. Am. Chem. Soc.* **1983**, *105*, 4800–4808; d) C. T. Walsh, Y.-C. J. Chen, *Angew. Chem.* **1988**, *100*, 342–352; *Angew. Chem. Int. Ed. Engl.* **1988**, *27*, 333–343; e) P. C. Brzostowicz, D. M. Walters, S. M. Thomas, V. Nagarajan, P. E. Rouvière, *Appl. Environ. Microbiol.* **2003**, 334–342; f) D. Sheng, D. P. Ballou, V. Massey, *Biochemistry* **2001**, *40*, 11156–11167.

[3] Reviews of enzymatic BV reactions: a) M. D. Mihovilovic, B. Müller, P. Stanetty, *Eur. J. Org. Chem.* **2002**, 3711–3730; b) J. D. Stewart, *Curr. Org. Chem.* **1998**, *2*, 195–216; c) S. D. Doig, L. M. O'Sullivan, S. Patel, J. M. Ward, J. M. Woodley, *Enzyme Microb. Technol.* **2001**, *28*, 265–274; d) J. D. Stewart, *Curr. Org. Chem.* **1998**, *2*,

195–216; e) S. Flitsch, G. Grogan, in: *Enzyme Catalysis in Organic Synthesis: A Comprehensive Handbook,* Vol. III, 2nd edn., (Eds.: K. Drauz, H. Waldmann) VCH, Weinheim, **2002**, p. 1202; f) N. M. Kamerbeek, D. B. Janssen, W. J. H. van Berkel, M. W. Fraaije, *Adv. Synth. Catal.* **2003**, *345*, 667–678; g) M. D. Mihovilovic, F. Rudroff, B. Grötzl, *Curr. Org. Chem*. **2004**, *8*, 1057–1069; h) J. D. Stewart, K. W. Reed, C. A. Martinez, J. Zhu, G. Chen, M. M. Kayser, *J. Am. Chem. Soc.* **1998**, *120,* 3541–3548.

[4] Synthetic applications of CHMOs in BV reactions:[3] a) M. J. Taschner, D. J. Black, *J. Am. Chem. Soc.* **1988**, *110*, 6892–6893; b) J. D. Stewart, K. W. Reed, J. Zhu, G. Chen, M. M. Kayser, *J. Org. Chem.* **1996**, *61*, 7652–7653; c) V. Alphand, R. Furstoss, S. Pedragosa-Moreau, S. M. Roberts, A. J. Willetts, *J. Chem. Soc. Perkin Trans. 1* **1996**, 1867–1872; d) M. D. Mihovilovic, B. Müller, A. Schulze, P. Stanetty, M. M. Kayser, *Eur. J. Org. Chem.* **2003**, 2243–2249; e) B. G. Kyte, P. Rouvière, Q. Cheng, J. D. Stewart, *J. Org. Chem.* **2004**, *69*, 12–17; synthetic applications of CHMOs in sulfoxidation: f) D. R. Light, D. J. Waxman, C. Walsh, *Biochemistry* **1982**, *21*, 2490–2498; g) G. Carrea, B. Redigolo, S. Riva, S. Colonna, N. Gaggero, E. Battistel, D. Bianchi, *Tetrahedron: Asymmetry* **1992**, *3*, 1063–1068; h) P. Pasta, G. Carrea, H. L. Holland, S. Dallavalle, *Tetrahedron: Asymmetry* **1995**, *6*, 933–936; i) V. Alphand, N. Gaggero, S. Colonna, R. Furstoss, *Tetrahedron Lett.* **1996**, *37*, 6117–6120; j) V. Alphand, N. Gaggero, S. Colonna, P. Pasta, R. Furstoss, *Tetrahedron* **1997**, *53*, 9695–9706; k) H. L. Holland, J.-X. Gu, A. Kerridge, A. Willetts, *Biocatal. Biotransform.* **1999**, *17*, 305–317; l) F. Secundo, G. Carrea, S. Dallavalle, G. Franzosi, *Tetrahedron: Asymmetry* **1993**, *4*, 1981–1982.

[5] a) M. T. Reetz, B. Brunner, T. Schneider, F. Schulz, C. M. Clouthier, M. M. Kayser, *Angew. Chem.* **2004**, *116*, 4167–4170; *Angew. Chem. Int. Ed.* **2004**, *43*, 4075–4078; b) M. T. Reetz, *Proc. Natl. Acad. Sci. USA* **2004**, *101*, 5716–5722.

[6] G. Chen, M. M. Kayser, M. D. Mihovilovic, M. E. Mrstik, C. A. Martinez, J. D. Stewart, *New J. Chem.* **1999**, *23*, 827–832.

[7] E. Malito, A. Alfieri, M. W. Fraaije, A. Mattevi, *Proc. Natl. Acad. Sci. USA* **2004**, *101*, 13157–13162.

[8] M. W. Fraaije, J. Wu, D. P. H. M. Heuts, E. W. van Hellemond, J. H. L. Spelberg, D. B. Janssen, *Appl. Microbiol. Biotechnol.* **2005**, *66*, 393–400.

[9] O. Lund, M. Nielsen, C. Lundegaard, P. Worning, *X3M: A Computer Program to Extract 3D Models*, Abstract at the CASP5 Conference, Livermore, California, USA, **2002**, A102.

[10] M. W. Fraaije, N. M. Kamerbeck, W. J. H. van Berkel, D. B. Janssen, *FEBS Lett.* **2002**, *518*, 43–47.

[11] a) M. T. Reetz, F. Daligault, B. Brunner, H. Hinrichs, A. Deege, *Angew. Chem.* **2004**, *116*, 4170–4173; *Angew. Chem. Int. Ed.* **2004**, *43*, 4078–4081; b) for earlier work on WT CHMO-catalyzed sulfoxidation, see refs.[3,4]

[12] V. Alphand, R. Furstoss, S. Pedragosa-Moreau, S. M. Roberts, A. J. Willetts, *J. Chem. Soc. Perkin Trans. 1* **1996**, 1867–1872.

[13] a) P. R. Gerber, K. Müller, *J. Comput.-Aided Mol. Des.* **1995**, *9*, 251–268; b) P. R. Gerber, *J. Comput.-Aided Mol. Des.* **1998**, *12*, 37–51; c) M. Bocola, N. Otte, K.-E. Jaeger, M. T. Reetz, W. Thiel, *ChemBioChem* **2004**, *5*, 214–223.

[14] Review of early models proposed by M. Taschner, R. Furstoss, G. Ottolina, S. Colonna, D. P. Kelly and others: a) A. Willetts, *Trends Biotechnol.* **1997**, *15*, 55–62; b) see also: S. Wang, M. M. Kayser, V. Jurkauskas, *J. Org. Chem.* **2003**, *68*, 6222–6228.

[15] a) F. H. Arnold, *Nature* **2001**, *409*, 253–257; b) K. A. Powell, S. W. Ramer, S. B. del Cardayré, W. P. C. Stemmer, M. B. Tobin, P. F. Longchamp, G. W. Huisman, *Angew. Chem.* **2001**, *113*, 4068–4080; *Angew. Chem. Int. Ed.* **2001**, *40*, 3948–3959; c) S. Brakmann, K. Johnsson, *Directed Molecular Evolution of Proteins (or How to Improve Enzymes for Biocatalysis)*, Wiley-VCH, Weinheim, **2002**; d) F. H. Arnold, G. Georgiou, *Directed Enzyme Evolution: Screening and Selection Methods*, in *Methods and Molecular Biology*, Vol. 230, Humana Press, Totowa, New Jersey, **2003**; e) A. Svendsen, *Enzyme Functionality – Design, Engineering and Screening*, Marcel Dekker, New York, **2004**; f) S. Brakmann, A. Schwienhorst, *Evolutionary Methods in Biotechnology (Clever Tricks for Directed Evolution)*, Wiley-VCH, Weinheim, **2004**.

[16] C.-S. Chen, Y. Fujimoto, G. Girdaukas, C. J. Sih, *J. Am. Chem. Soc.* **1982**, *104*, 7294–7299.

